Braz J Phys (2012) 42:237–247
DOI 10.1007/s13538-012-0081-2

NUCLEAR PHYSICS

Axial Neutron Flux Evaluation in a Tokamak System: a Possible Transmutation Blanket Position for a Fusion–Fission Transmutation System

Carlos E. Velasquez · Graiciany de P. Barros · Claubia Pereira · Maria A. Fortini Veloso · Antonella L. Costa

Received: 28 August 2011 / Published online: 17 May 2012

Abstract A sub-critical advanced reactor based on Tokamak technology with a D–T fusion neutron source is an innovative type of nuclear system. Due to the large number of neutrons produced by fusion reactions, such a system could be useful in the transmutation process of transuranic elements (Pu and minor actinides (MAs)). However, to enhance the MA transmutation efficiency, it is necessary to have a large neutron wall loading (high neutron fluence) with a broad energy spectrum in the fast neutron energy region. Therefore, it is necessary to know and define the neutron fluence along the radial axis and its characteristics. In this work, the neutron flux and the interaction frequency along the radial axis are evaluated for various materials used to build the first wall. W alloy, beryllium, and the combination of both were studied, and the regions more suitable to transmutation were determined. The results demonstrated that the best zone in which to place a transmutation blanket is limited by the heat sink and the shield block. Material arrangements of W alloy/W alloy and W alloy/beryllium would be able to meet the requirements of the high fluence and hard spectrum that are needed for transuranic transmutation. The system was simulated using the MCNP code, data from the *ITER Final Design Report*, *2001*, and the Fusion Evaluated Nuclear Data Library/MC-2.1 nuclear data library.

Keywords Fusion · Fission · Transmutation

C. E. Velasquez · G. de P. Barros · C. Pereira (✉) · M. A. Fortini Veloso · A. L. Costa
Departamento de Engenharia Nuclear, Universidade Federal de Minas Gerais,
Av. Antonio Carlos, 6627 campus UFMG,
31.270-90, Belo Horizonte, MG, Brazil
e-mail: claubia@nuclear.ufmg.br

C. E. Velasquez
e-mail: carlosvelcab@eng-nucl.mest.ufmg.br

G. de P. Barros
e-mail: gbarros@ufmg.br

M. A. Fortini Veloso
e-mail: dora@nuclear.ufmg.br

A. L. Costa
e-mail: antonella@nuclear.ufmg.br

C. E. Velasquez · G. de P. Barros · C. Pereira · M. A. Fortini Veloso · A. L. Costa
Instituto Nacional de Ciência e Tecnologia de Reatores Nucleares Inovadores/CNPq, Rede Nacional de Fusão (FINEP/CNPq),
Rio de Janeiro, Brazil

1 Introduction

Advanced reactor concepts based on generation IV nuclear energy systems have been proposed to reduce the quantity of waste produced in current commercial reactors by the partition and transmutation of plutonium (Pu) and minor actinides (MAs) [1]. A hybrid fusion–fission reactor is one of the options among the proposed systems [2, 3]. In 2008, the Brazilian government commissioned two new institutions, the *Instituto Nacional de Ciências e Tecnologia de Reatores Nucleares Inovadores/CNPq* and the *Rede Nacional de Fusão/FINEP*, to study new-generation reactor designs and systems. The *Departamento de Engenharia Nuclear/UFMG*, in partnership with these two institutions, has also developed models of fusion- and accelerator-driven systems to study Pu and MA transmutation [4, 5] considering that subcritical systems have criticality and safety advantages [6–8].

The aim of this work is to extend our previous study [4] by evaluating the axial neutron flux in the system based on

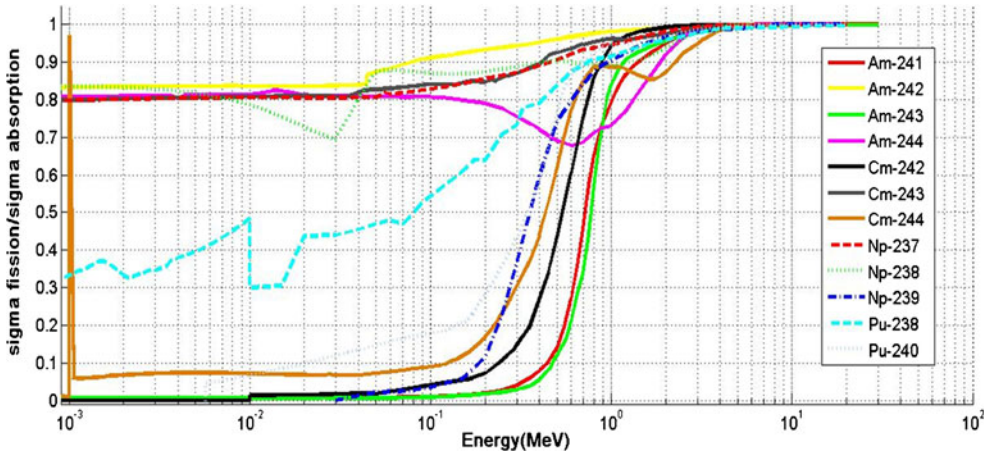

Fig. 1 (*Color online*) Fission-to-total absorption ($\sigma_f/(\sigma_f+\sigma_\gamma)$) probabilities of transuranic nuclides [26]

the International Thermonuclear Experimental Reactor (ITER) concept and to determine possible positions to insert the transmutation layer. As the transuranics (TRU) have larger fission-to-capture ratios in a fast spectrum than in a thermal spectrum, the goal is to choose the region in which the neutron flux is harder, increasing the transuranics' transmutation probabilities. Different materials have been proposed for the first wall ITER composition [9–11]. These materials have desirable properties, such as a high melting point, high thermal conductivity, and high resistances to sputtering, particle fluencies, and erosion [9, 12–14]. Tungsten fulfils these requirements and is the main component in several alloys. Therefore, W alloys are considered for several plasma-facing components [15, 16]. The main reasons to select beryllium are based on its acceptable effect on plasma performance, resistance to thermal cyclic loading under neutron irradiation conditions, properties as a neutron multiplier and high oxygen gettering characteristics [17, 18]. Therefore, W alloy, beryllium and the combination of both are used in this paper. The goal is to predict the best position to add a transmutation blanket according to the different materials used. To enhance the transmutation efficiency, it is necessary to have a high neutron wall loading (high neutron fluence) with a broad energy spectrum in the fast neutron energy region. [12]

The simulations were performed using the Monte Carlo N-particle (MCNP) code [19], data from the ITER Final Design Report 2001 [20], and the Fusion Evaluated Nuclear Data Library data library [21]. Using these results, the neutron behaviour for each material can be compared to find a suitable region with a high neutron fluence and hard spectrum.

2 Fusion–Fission Transmutation System

2.1 Transuranics Transmutation (Pu and Minor Actinides)

To reduce the environmental impact of long-term geological repositories, the concepts of separation and transmutation have been introduced. Separation refers to the process of separate storage of fission products that emit high-energy decay products (alpha, beta, and gamma) until their high level of radioactivity decays away. Transmutation refers to reprocessing the spent fuel that is discharged from light water reactors (LWRs) and separating the long-lived fissionable TRUs for use as fuel [7]. The concept of separating

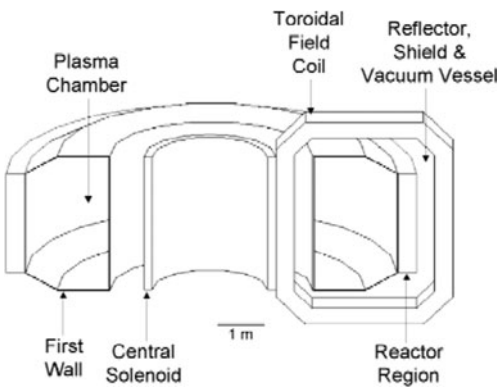

Fig. 2 Schematic of the geometric configuration of the FTWR [2]

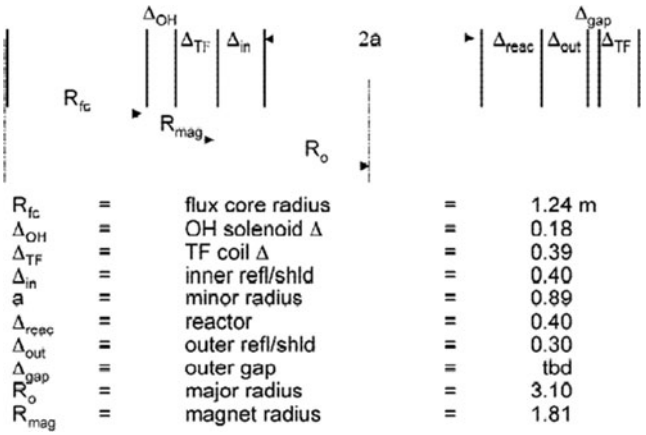

Fig. 3 Radial build of the FTWR [2]

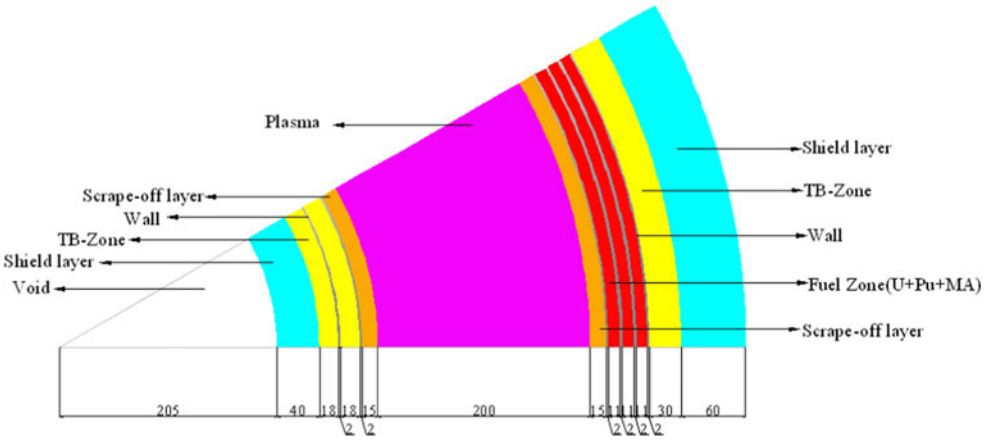

Fig. 4 (*Color online*) Radial configuration of the FDS-EM [3]

TRUs from the spent nuclear fuel that is discharged from LWRs for use as fuel in fast and thermal reactors for reduction of the long-lived TRU isotopes was investigated, and the relevant studies concluded that it is possible to reduce these isotopes significantly (>90 %). Therefore, it was concluded that subcritical reactors could operate with highly burned fuel or with fuel consisting of MAs to achieve >>90 % burnup of the TRUs [7, 22, 23]. In this work, we are interested in the possibility of Pu and MA (americium, curium, and neptunium) transmutation in a fusion–fission system.

Although fission products have a significant risk of radiotoxicity for the first few hundred years, the main contribution over thousands of years is due to the actinides [24, 25]. Because all actinides are potentially radiotoxic and because neutron capture (n, γ) reactions in the actinides only produce other actinides, neutron fission (n, f) reactions are a more effective way to burn up actinides. Figure 1 shows the plutonium and MA fission-to-total absorption probabilities ($\sigma_f/(\sigma_f+\sigma_\gamma)$) [26]. The long-term radiotoxic inventory in the spent fuel discharged from LWRs can be reduced considerable by using the multirecycling strategy in advanced pressurised water reactors (PWRs); this strategy primarily reduces ^{239}Pu, ^{241}Pu, ^{242}Am, ^{244}Am, ^{237} Np, ^{238} Np, and ^{243}Cm, which can be partly transmuted in a thermal-neutron spectrum, as shown in Fig. 1. However, some of the actinides are effectively nonfissionable in a thermal–neutron spectrum (Fig. 1; ^{241}Am, ^{243}Am, ^{242}Cm, ^{244}Cm, ^{239}Np, and ^{240}Pu). Therefore, to achieve transmutation, high-energy neutrons that are released from fusion reactions must enter into a subcritical blanket containing Pu and MAs, increasing the probability for these neutrons to induce transmutation reactions.

Table 1 ITER parameters [28]

Parameters	ITER
Major radius of plasma (m)	6.21
Minor radius of plasma (m)	2.0
Volume of plasma (m^3)	837
Plasma current (MA)	15
P_{NB} (MW)	33–50
P_{RF} (MW)	20–40
Magnetic field (T)	5.3
Duration of pulses (s)	>400 s
Type of plasma	D–T
Thermonuclear power (Pth)	500 MW
Fusion energy (GJ)	>120
Electron temperature (keV)	21
Ion temperature (keV)	18
$Q=P_{th}$/heating power	>10
Neutron power at the edge	0.57 MW/m²

2.2 Different Models of Blanket Design

Many studies have been conducted around the world with the purpose of developing a transmutation blanket design. Some of the most representative works are in development in the USA and China.

2.2.1 The USA's Blanket Design

The geometric configuration of the fusion transmutation of waste reactor is shown in Figs. 2 and 3. The transmutation reactor consists of a 40-cm-thick ring of vertical hexagonal fuel assemblies located outboard of the plasma chamber of a tokamak fusion neutron source. The reactor's metallic fuel consists of a zirconium alloy containing transuranics from spent nuclear fuel that are dispersed in a zirconium matrix and clad with steel that is similar to HT-9. The coolant for the reactor, reflector and shield, first wall, and divertor is eutectic Li17Pb83 that is enriched to 20 % ^{6}Li to meet the tritium self-sufficiency requirement. The reflector and shield are located inboard of, above, and below the plasma chamber and above, below, and outboard of the reactor to protect the magnets from radiation damage and to reflect neutrons towards the reactor. The toroidal and poloidal magnets

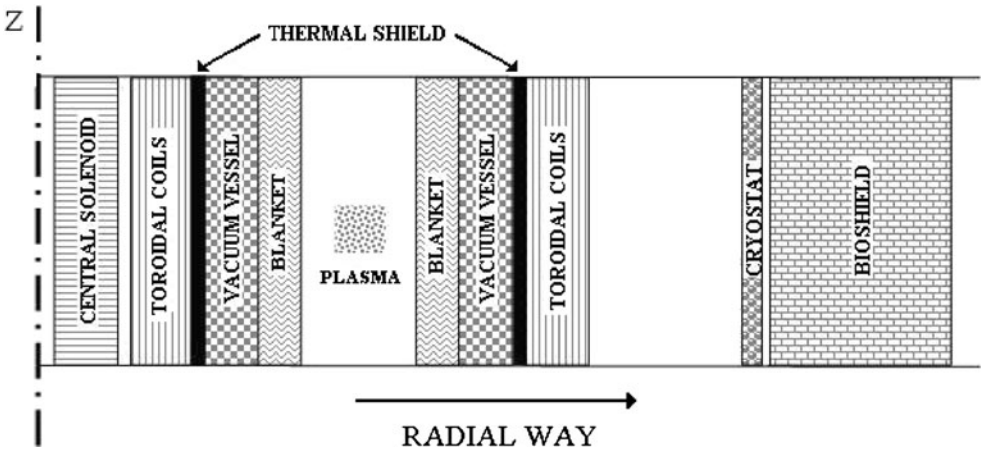

Fig. 5 Radial 1D model profile (scale out). *Blank spaces* vacuum areas

employ an oxygen-free high conductivity copper conductor and liquid nitrogen coolant [2].

2.2.2 China's Blanket Design

The general design of the Fusion Driven System-EM utilises a subcritical blanket that interacts with the copious fusion neutrons that are provided by the fusion core to achieve tritium breeding and energy multiplication based on the fission and fusion fuel cycle (Fig. 4). The design of the blanket system is based on the well-developed technologies of pressurised water reactors. In addition to the shielding modules, two types of functional blanket modules, the tritium breeding module and the fission energy production module (EPM), are designed for the inner board, which is only used to breed tritium, and the outer board, which is used to produce energy with fission materials, respectively.

The fission materials in the blanket of the EPM are composed of depleted uranium, which serves as the fissile fuel breeding material, and plutonium isotopes, which serve as neutron multipliers with long-lived MA, i.e., ^{237}Np, ^{241}Am, ^{243}Am, and ^{244}Cm. Adapting spent fuel directly from commercial power plants (e.g., PWR) for this use avoids the difficult process of separating these isotopes. The dioxide fuel form is adopted to palliate the reprocessing technology of the spent fuel [3].

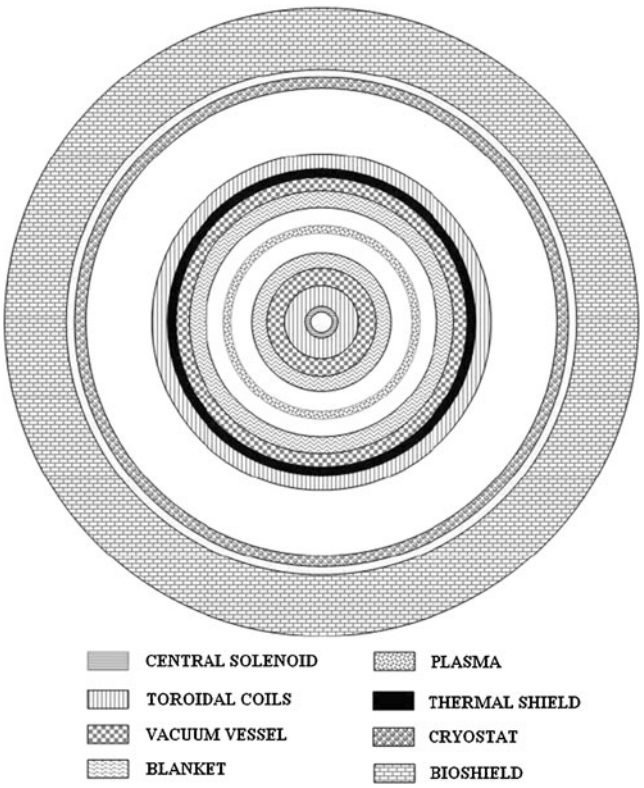

Fig. 6 Top view of geometric model (scale out). *Blank spaces* vacuum areas

2.3 Plasma Parameters

ITER is an experimental device design with extensive diagnostics and considerable flexibility in plasma shaping, heating and current drive, and fuelling methods. ITER aims to operate in a range of plasma scenarios characterised by different maximum plasma currents, shape parameters, additional heating strategies, and plasma current density profiles. A fusion neutron source based on ITER physics and technology would be capable of generating up to 500 MW (thermal) of fusion power. Details of the modelling used are presented in the methodology section. Table 1 shows some of the experiments performed with the Tokamak parameters and the parameters expected for the ITER.

The first wall is an important focus of investigation by researchers around the world because it is subjected to extreme conditions during operation. This wall must have desirable properties such as a high melting point, high thermal conductivity, and high resistances to sputtering, particle fluencies, and erosion [12–14]. The different proposed materials that have been studied are tungsten, which was tested by the ASDEX upgrade (Germany) [9],

Table 2 Materials and thicknesses adopted for the simulated component models

Component		Thickness (cm)	Material
CS	Insertion module	80 a 90	27 % Nb_3Sn+30 % Incoloy 908+30 % SS316+10 % resins+ 3 % Al_2O_3
	Superconductor and insulator	90 a 180	45 % Nb_3Sn+5 % Al_2O_3+ 50 % Incoloy 908
	Support	180 a 200	SS316L(N)IG
TFC	Wall box	220 a 229.5	SS316L(N)IG
	Superconductor and insulator	229.5 a 310.5	45 % Nb_3Sn+5 % Al_2O_3+ 50 % Incoloy 908
	Wall box	310.5 a 320	SS316L(N)IG
VVTS	Wall	320.6 a 322.8	SS304L
VV	Wall	322.8 a 328.8	SS316L(N)IG
	Filling	328.8 a 350.5	SS304B7, 60 %; water, 40 %
	Wall	350.5 a 356.5	SS316L(N)IG
BLK	Shield block	357 a 399	SS316L(N)IG
	Heat sink	399 a 401	CuCrZr-IG
	First wall	401 a 402	Material to be studied
Plasma chamber		402 a 853	Vacuum
BLK	First wall	853 a 854	Material to be studied
	Heat sink	854 a 856	CuCrZr-IG
	Shield block	856 a 898	SS316L(N)IG
VV	Wall	898.5 a 904.5	SS316L(N)IG
	Filling	904.5 a 967.5	SS304B7, 60 %; water, 40 %
	Wall	967.5 a 973.5	SS316L(N)IG
VVTS	Wall	973.5 a 975.5	SS304L
TFC	Wall box	976 a 985.5	SS316L(N)IG
	Superconductor and insulator	1085.5 a 1165.5	45 % Nb_3Sn+5 % Al_2O_3+ 50 % Incoloy 908
	Wall box	1165.5 a 1176	SS316L(N)IG
CRY	Wall	1400 a 1410	SS304L
BSD	Wall	1455 a 1655	Concrete

BLK blanket, *VV* vacuum vessel, *VVTS* vacuum vessel thermal shield, *TFC* toroidal field coils, *CRY* cryostat, *BSD* bioshield

beryllium, which was recently tested by JET (England) [10], and molybdenum, which was tested by Alcator-Mod (USA) [11]. In this work, tungsten, beryllium, and the combination of both are evaluated as a first-wall material.

Table 3 Concrete composition used

Elements	Composition (ρ=2.43 gcm^{-3})
H	0.4532
B	0.07
O	51.2597
Na	1.1553
Mg	0.3866
Al	3.5548
Si	35.9664
K	1.4219
Ca	4.3546
Fe	1.3775

3 Methodology

The modelling technique used in this work was the same as that adopted by Araujo et al. [4], and it will be described in the next section.

3.1 Geometric Model

The geometric model used concentric finite cylinders, as shown in Fig. 5. The cylindrical surfaces are 24 m high and have the same axial alignment. Each region between two successive cylindrical surfaces was filled with the appropriate material to represent the different layers of each component along the radial reactor direction.

This simplified model disregards the details of components that are more complex, omits the vertical and horizontal slits between blanket modules, and does not consider components that do not involve the whole machine. The top view of the geometry used in the modelling is shown in Fig. 6.

3.2 Materials

The MCNP code models the transport of neutrons, photons, and electrons or the combined transport of these particles, where the random path of the particles is simulated based on stochastic laws, and the interaction probability is inserted from libraries of nuclear cross sections. The accuracy obtained with the MCNP simulation depends on several uncertainties involved in the nuclear cross-section data and the uncertainty of the statistical calculation. Therefore, the details of the material composition for each reactor component are highly relevant to obtain a reliable prediction of the individual history of each neutron in the simulation.

Table 2 presents the reactor systems used in this study with the thickness and materials for each: central solenoid (CS), blanket, vacuum vessel, vacuum vessel thermal shield, toroidal field coils, cryostat, and bioshield.

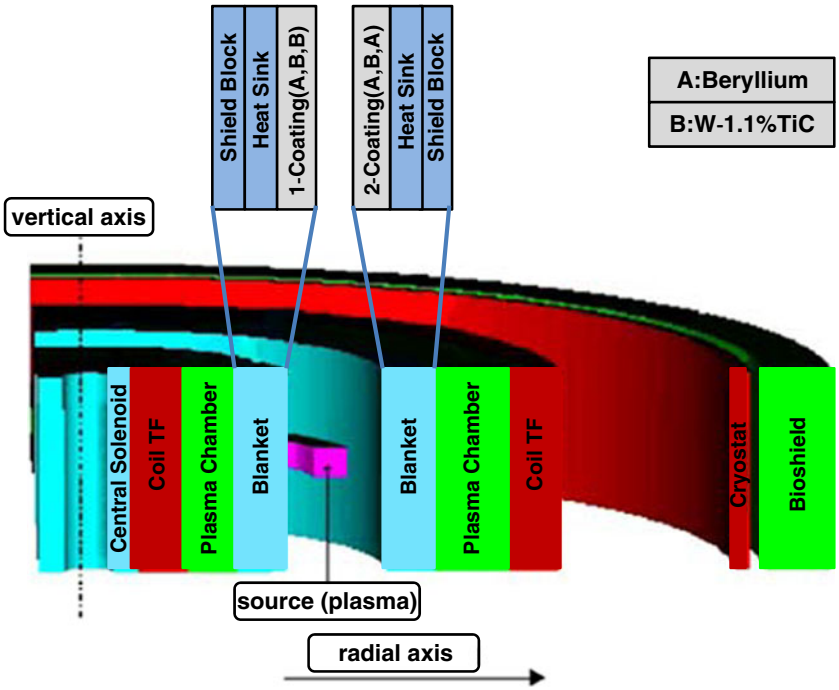

Fig. 7 (*Color online*) System blanket design

The material of the first wall located inside the blanket is the focus of this study.

In agreement with ITER guidelines and the article in fusion engineering and design [15, 16], stainless steel SS316L(N)IG was used at the filling material in the blanket shield block. The vacuum vessel was 60 % filled with stainless steel SS304B7 and 40 % filled with water. Due to the CS composition complexity, this module's composition was assumed to be 27 % Nb_3Sn+30 % Incoloy 908+30 % SS316+10 % resins+3 % Al_2O_3. To simplify the model, the small details of the CS composition were not considered. The composition of the filling material of the CS and TF coils was assumed to be 45 % Nb_3Sn+50 % Incoloy 908+5 % Al_2O_3. The composition of the bioshield is described in Table 3.

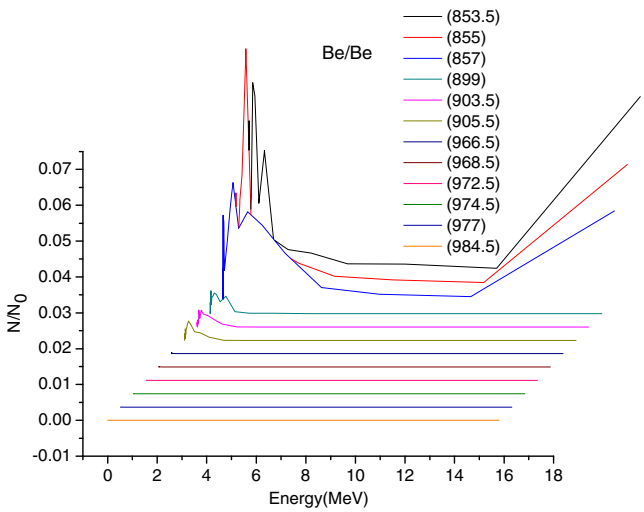

Fig. 8 *(Color online)* Neutron spectrum for the Be–Be coating

To evaluate the neutron flux in different materials based on the Tokamak design, the coatings surrounding the fusion plasma were changed (Fig. 7). To help us understand the reactions that occur along the neutron trajectory for each blanket, the different reaction rates were tracked. In the first experiment, beryllium was placed in the 1 and 2 coating positions surrounding the fusion plasma because beryllium is an excellent neutron multiplier. However, W and W alloys (W-1.1TiC) [12] are being considered due to the desirable structural properties of

Table 4 Interaction frequencies for each type of reaction for Be/Be

Distance (cm)	Reaction type	Interaction frequency (particles/s)	Normalised
853.5	Elastic collision	1.87659E+09	0.89118
	Inelastic collision	6.34246E+05	3.01199E-4
	Radiative capture	8.00067E+04	3.79946E-5
	Neutron production	1.62307E+05	7.70784E-5
	Total cross section	2.10574E+09	1
855	Elastic collision	8.78642E+08	0.68332
	Inelastic collision	1.46913E+08	0.11425
	Radiative capture	3.42448E+06	0.00266
	Neutron production	1.53811E+08	0.11962
	Total cross section	1.28585E+09	1
857	Elastic collision	3.36108E+08	0.60728
	Inelastic collision	9.937732E+07	0.1786
	Radiative capture	7.44902E+05	0
	Neutron production	4.79211E+07	0.08543
	Total cross section	5.52983E+08	1

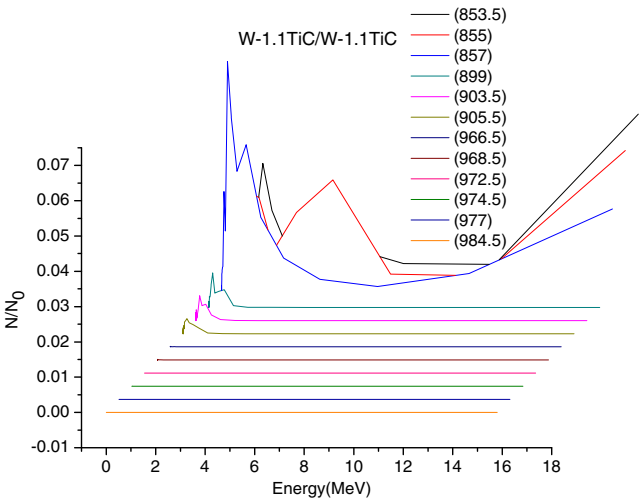

Fig. 9 (*Color online*) Neutron spectrum for the W1.1TiC/W1.1TiC coating

tungsten: its high melting point, high thermal conductivity, and high resistance to sputtering and erosion.

In the second experiment, the beryllium coating was replaced with a tungsten alloy (W-1.1TiC) material in the 1 and 2 coating positions to verify the different reactions due to the neutron production induced by fusion reactions. To compare and evaluate the neutron multiplier parameters, the last experiment used a combination of both materials; the tungsten alloy (W-1.1TiC) was used in the 1 coating position, and beryllium was used in the 2 coating position. The neutron fluence was measured along the radial axis for both materials using tally point detectors from the MCNP code. Detectors

Table 5 Interaction frequencies for each type of reaction for W1.1TiC/W1.1TiC

Distance (cm)	Reaction type	Interaction frequency (particles/s)	Normalised
853.5	Elastic collision	3.08081E+09	0.70764
	Inelastic collision	8.24294E+07	0.01893
	Radiative capture	3.45950E+07	0.00795
	Neutron production	8.13846E+05	1.86935E-4
	Total cross section	4.35363E+09	1
855	Elastic collision	8.19653E+08	0.70964
	Inelastic collision	1.19205E+08	0.10321
	Radiative capture	2.54904E+06	0.00221
	Neutron production	1.27194E+08	0.11012
	Total cross section	1.15503E+09	1
857	Elastic collision	3.17346E+08	0.63917
	Inelastic collision	8.193039E+07	0.16418
	Radiative capture	5.55145E+05	0
	Neutron production	3.96457E+07	0.07887
	Total cross section	4.96187E+08	1

Table 6 Data changed for the new design

Centre		0	Vacuum
Blanket	Shield block	357 a 399 cm	SS316L(N)IG
	Heat sink	399 a 401 cm	CuCrZr-IG
	First wall	401 a 402 cm	W-1.1TiC
Plasma chamber		402 a 853 cm	Vacuum
Blanket	First wall	853 a 854 cm	Beryllium
	Heat sink	854 a 856 cm	CuCrZr-IG
	Shield block	856 a 898 cm	SS316L(N)IG

were placed before and after each blanket in the radial direction starting with the 2 coating position. The spectrum energy width is needed to identify possible positions for a transmutation blanket. The combinations of coating materials evaluated were beryllium (1 coating) and beryllium (2 coating), W-1.1TiC (1 coating) and W-1.1TiC (2 coating), and W-1.1TiC (1 coating) and beryllium (2 coating).

3.3 Fusion Neutron Source

The fusion neutron source used is isotropic, has a ring shape with a square cross-section that is 0.60 m high and 0.60 m wide, and occupies the central part of the plasma chamber. This source does not take into account the plasma emission asymmetries in the poloidal and toroidal directions. The energy distribution for the fusion neutron source is described by a Gaussian fusion energy spectrum that obeys the Gaussian distribution:

$$p(E) = C\ \exp[-((E-b)/a)2],$$

where a is the width in MeV and b is the average energy in milli-electron volt. The parameters of the emission spectrum

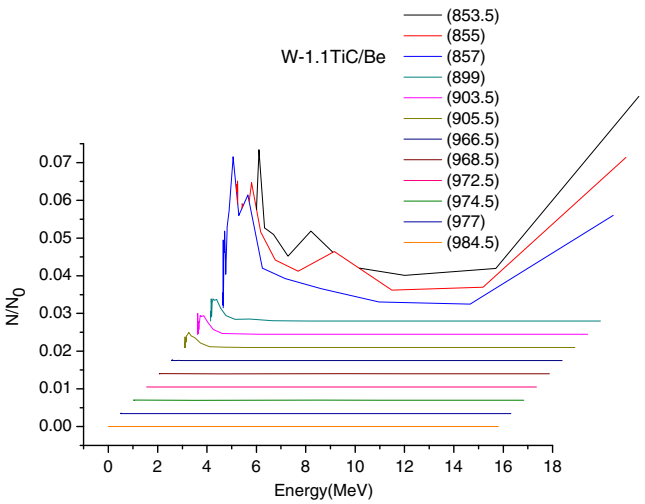

Fig. 10 (*Color online*) Neutron fluence results for the W–Be arrangement

Table 7 Interaction frequencies for each type of reaction for WTiC/Be

Distance (cm)	Reaction type	Interaction frequency (particles/s)	Normalised
853.5	Elastic collision	1.74528E+09	0.88536
	Inelastic collision	2.23634E+05	1.13447E-4
	Radiative capture	7.18623E+04	3.6455E-5
	Neutron production	3.30068E+04	1.6744E-5
	Total cross section	1.97126E+09	1
855	Elastic collision	9.29500E+08	0.69768
	Inelastic collision	1.44866E+08	0.10874
	Radiative capture	3.63000E+06	0.00272
	Neutron production	1.52679E+08	0.1146
	Total cross section	1.33228E+09	1
857	Elastic collision	4.12944E+08	0.65715
	Inelastic collision	9.967599+07	0.15777
	Radiative capture	7.08024E+05	0
	Neutron production	4.54232E+07	0.07128
	Total cross section	6.28018E+08	1

were adjusted automatically by MCNP through the choice of a standard source for D–T fusion. The plasma temperature was chosen to be 10 keV [19]. Considering the aims of this study, such simplifications are acceptable.

4 Results and Analysis

4.1 Neutronic Evaluation of Different Coating Materials

For each case, the neutron fluence (N) measured by the detectors were divided by the initial neutron fluence (N_0) measured

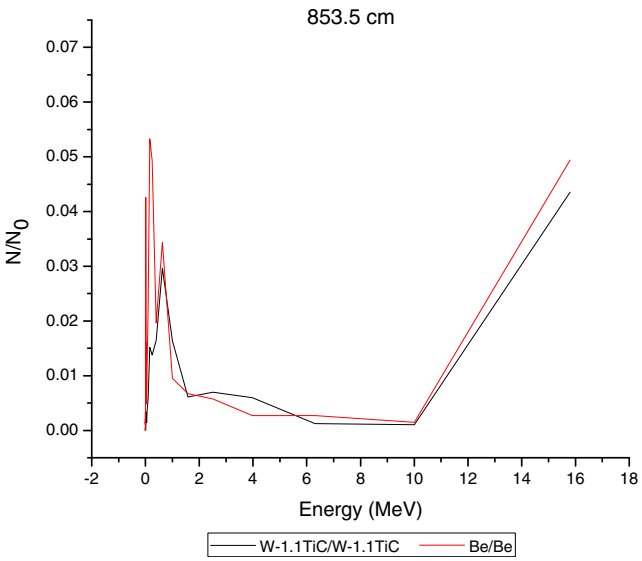

Fig. 11 (*Color online*) Comparison between beryllium and tungsten at 853.5 cm

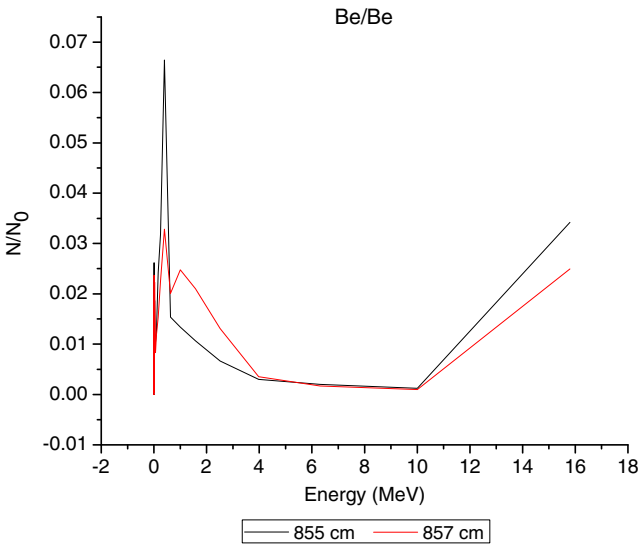

Fig. 12 (*Color online*) Neutron fluence at 855 and 857 cm from the centre

at the neutron source location. Therefore, the quantity N/N_0 is used in the analysis to study the rate of change in the neutron population that passes through the walls. To better understand the reactions that occur, the interaction frequencies for the different reaction cross-sections along the radial axis were recorded. The following reaction cross were sections considered: elastic collision, inelastic collision, radiative capture, neutron production, and total. For each distance, the reaction cross-section was normalised with respect to the total cross-section to determine that reaction's contribution to the total.

4.1.1 The Effect of a Beryllium Coating

In the first case, a beryllium coating surrounding the fusion plasma chamber was considered. The results are shown in

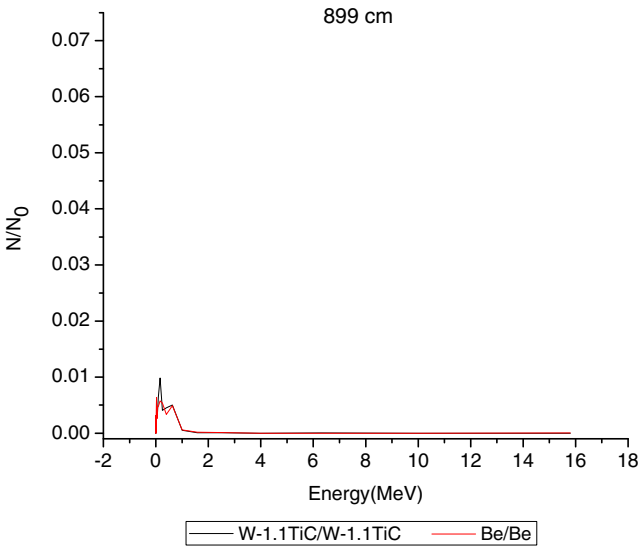

Fig. 13 (*Color online*) Neutron fluence at 899 cm from the centre

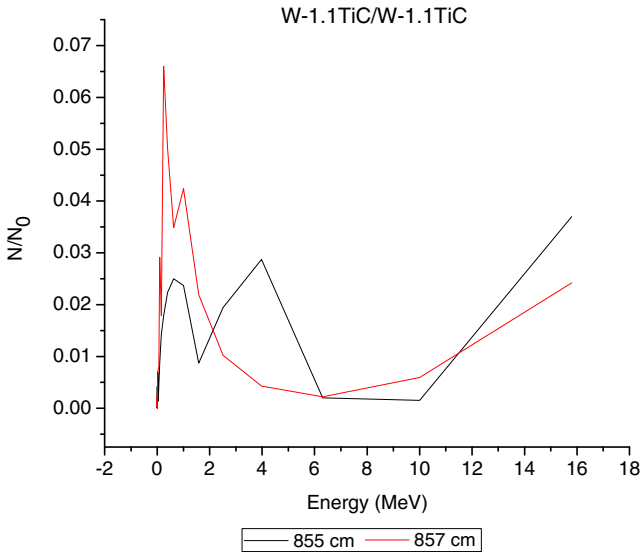

Fig. 14 (*Color online*) Neutron fluence at 855 and 857 cm from the centre

Fig. 8, which shows the neutron fluence measured along the radial axis for each chosen distance.

Figure 8 shows a high intensity at 855 cm from the centre, where the second detector is located (heat sink, see Table 2). The peak denotes a high neutron production but is missing a broader energy spectrum. However, the next relevant zone, located at 857 cm, has a broader energy spectrum and a significant neutron fluence indicating that this zone is suitable to place a transmutation blanket. Table 4 presents the types of reactions and their interaction frequencies at three distances.

4.1.2 The Effect of a Tungsten Alloy Coating

In the second case, a tungsten coating surrounded the plasma chamber. In recent evaluations [27], the tungsten alloy was considered for various plasma-facing components; the evaluations indicate that tungsten alloy could be a suitable option for replacing the beryllium.

Two important peaks can be identified in the results in Fig. 9; the first peak is located inside the heat sink at 855 cm, and the second peak is inside the shield block at 857 cm. Therefore, a suitable region to place a transmutation blanket would be limited to these two regions. Table 5 presents the types of reactions and their interaction frequencies at three distances.

4.1.3 The Effect of Tungsten and Beryllium Coatings

As shown in Figs. 8 and 9, beryllium has a greater neutron fluence but a narrower energy spectrum when compared to the tungsten at 855 cm. However, the tungsten alloy has a greater neutron fluence with the same width as the beryllium at 857 cm. Therefore, it is interesting to evaluate the feasibility of using both materials. For this last case, coatings of both materials were placed as shown in Table 6. This arrangement was considered due to the evaluated properties of each material: the tungsten alloy had greater absorption and inelastic reaction rates than beryllium (Table 3). The tungsten alloy was placed in the inner position and, due to its multiplier features, the beryllium was more appropriately placed in the outer position surrounding the plasma vacuum, as shown in Table 5.

As seen in Fig. 10, the region exhibiting a high neutron fluence and broad energy spectrum was located between 855 and 857 cm, limited by the heat sink and the protector block. According to these preliminary results, a suitable area to place a transmutation blanket that meets the main requirements could be between 855 and 857 cm. These results show that the W1.1TiC/Be arrangement (located as shown in Table 5) is a suitable coating option. Table 7 presents the types of reactions and their interaction frequencies for three distances.

4.2 A Detailed Analysis

The following results present the most relevant fluence peaks associated with a suitable position for a transmutation blanket for the different studied cases.

4.2.1 Beryllium

As shown in Fig. 11, the neutron fluence through beryllium was greater than the fluence through tungsten. Based on the reaction cross-sections in Tables 4 and 5 and Fig. 11, this

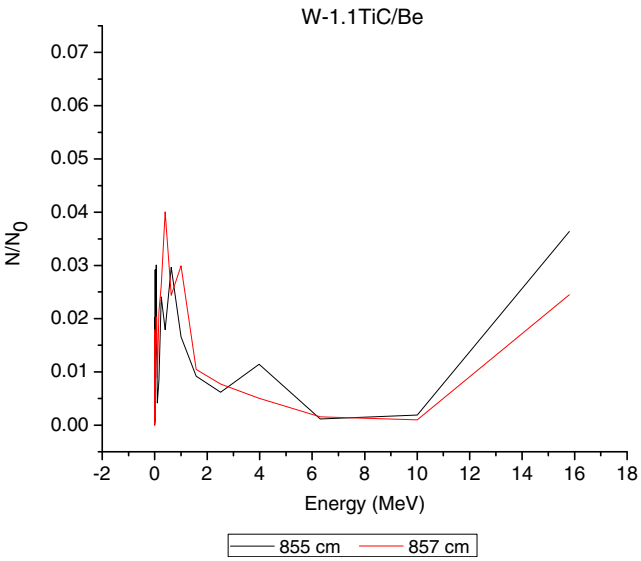

Fig. 15 (*Color online*) Neutron fluence at 857 cm from the centre in the shield block

fluence difference is due to the larger reaction rate in the tungsten alloy than in the beryllium material.

As illustrated in Fig. 8, there are two relevant peaks. The first peak is located 855 cm from the centre, where the highest neutron fluence occurs; this peak has a fluence of 0.065 times the initial fluence and an energy spectrum width between 0.0398 and 0.631 MeV. The second peak is at approximately 857 cm. As seen in Fig. 12, this peak has a lower neutron fluence than the first peak but has a broader energy spectrum between 0.0398 and 3.98 MeV, showing this location to be a suitable zone. However, the abrupt decrease in the neutron fluence from 855 to 857 cm and the large deficiency in the energy spectrum width limited the probability of transmutation. Therefore, although this region is the best choice for placement of a transmutation blanket, the results do not satisfy the main requirements.

4.2.2 Tungsten Alloy

This evaluation was performed for the tungsten alloy coating. First, to obtain a better idea of the fluence behaviour away from the centre, the beryllium and tungsten–alloy cases were compared. In Figs. 8 and 9, the most representative peaks were located at 899 cm. Therefore, Fig. 13 presents the neutron fluence at 899 cm for beryllium and the tungsten alloy. In both cases, the neutron fluence to achieve transmutation is low (<0.01), and the energy spectrum width is between 0.00631 and 1 MeV. However, the main analysis will be focused on the regions with larger neutron fluences (from 855 to 857 cm), as shown in Fig. 9.

Figure 14 shows a peak with a high neutron fluence at 855 cm. The neutrons with high energies between 2 and 6 MeV lose energy when they pass through the heat sink (855 cm) to the shield block (857 cm). Between 0.158 and 2 MeV, a large fluence of approximately 0.065 is observed at 857 cm from the centre. This abrupt change in energy is due to the increase in the inelastic reaction rate as the neutron passes through the heat sink at 855 cm. Therefore, a suitable zone in which to place a transmutation blanket could be located between these two regions (heat sink and shield block).

4.2.3 Tungsten/Beryllium Coating

This coating uses tungsten in the inner position and beryllium in the outer one, as indicated in Table 6. According to the calculation results (Fig. 10), the maximum neutron fluence was 0.04 at 857 cm, and the width of interest was from 0.1 to 1.58 MeV. This region between the heat sink (855 cm) and the shield block (857 cm) is a suitable zone in which to place a transmutation blanket due to the combination of a high fluence and a larger energy spectrum width (Fig. 15).

According to the last results, the zone between the heat sink and the protector block could be a suitable solution for a transmutation blanket position because it accomplishes the requirements of neutron flux (broad energy spectrum and high fluence), allowing the transmutation of nuclear waste.

5 Conclusions

This work represents our initial efforts to simulate a Tokamak based on the ITER blanket distribution using MCNP. The results suggest the best position to add a transmutation blanket based on the neutronic evaluation and the material's behaviour. Some coating combinations were examined for the first wall. The evaluated cases demonstrated that the best zone in which to place a transmutation blanket is limited by the heat sink and the shield block. Material arrangements of W alloy/W alloy and W alloy/beryllium would be able to meet the requirements of high fluence and broad energy spectrum. These arrangements are expected to achieve transmutation, maintaining a subcritical state $k_{\text{eff}}<0.99$. The next step is to design a transmutation blanket and study the behaviour of the transuranic elements under the conditions presented here. Additionally, introducing a transmutation layer and simulating this system using a depletion code would be useful to analyse the transmutation layer evolution during operation time.

Acknowledgments The authors are grateful to CNEN, CAPES, CNPq and FAPEMIG (Brazil) for their support.

References

1. Commissariat à l´énergie atomique, *"Nuclear energy of the future: what research for which objective?"*, *e-den*,CEA, (2006)
2. W.M. Stacey et al., A fusion transmutation of waste reactor. Fusion Sci. Technol. **41**, 116–140 (2002)
3. Y. Wu et al., The fusion–fission hybrid reactor for energy production: a practical path to fusion application. http://www-pub.iaea.org/mtcd/meetings/fec2008/ft_p3-21.pdf
4. A. Araujo, C. Pereira, M.A.F. Veloso, A.L. Costa, Flux and dose rate evaluation of iter system using MCNP5. Braz. J. Phys. **40**, 58–62 (2009)
5. G.P. Barros, C. Pereira, M.A.F. Veloso, A.L. Costa, Neutron production evaluation from a ADS target utilizing the MCNPX 2.6.0 code. Braz. J. Phys. **40**(4), 414–418 (2010)
6. J.W. Maddox, W.M. Stacey, Fuel cycle analysis of a subcritical fast helium-cooled transmutation reactor with a fusion neutron source. Nucl. Technol. **158**(1), 94–108 (2006)
7. C.M. Sommer, W.M. Stacey, Fuel cycle analysis of the SABR subcritical transmutation reactor concept. Nucl. Tech. **172**, 48–59 (2010)

8. E.A. Hoffman, W.M. Stacey, Comparative fuel cycle analysis of critical and subcritical fast reactor transmutation systems. Nucl. Technol. **144**, 83–121 (2003)
9. R. Neu et al., Operational conditions in a W-clad tokamak. J. Nucl. Mater. **367–370**, 1497–1502 (2007)
10. M. J. Rubel et al., Beryllium plasma-facing components for the ITER-like Wall Project at JET. J. Phys.: Conf. Ser. **100**, 062028 (2008)
11. W.R. Wampler, Molybdenum erosion measurements in Alcator C-Mod. J. Nucl. Mater. **266–269**, 217–221 (1999)
12. A. Robinson, L. El Guebaly, D.Henderson, *W-Based Alloys for Advanced Divertor Designs: Detailed Activation and Radiation Damage Analysis*, Fusion Technology Insitute, University of Wisconsin, October (2010)
13. M.R. Gilbert, J-Ch Sublet, Neutron-induced transmutation effects in W and W-alloys in a fusion environment. Nucl. Fusion **51**, 1–13 (2011)
14. H. Maier et al., Tungsten and beryllium armour development for the JET ITER-like wall project. Nucl. Fusion **47**, 222–227 (2007)
15. R. Pampin, Tungsten transmutation and resonance self-shielding in PPCS models for the study of sigma-phase formation, *UKAEA FUS 525*, EURATOM/UKAEA Fusion, (2005)
16. M. Kaufmann, R. Neu, Tungsten as first wall material in fusion devices. Fusion Eng. Des. **82**, 521–527 (2007)
17. T.A. Tomberlin, *Beryllium—a unique material in nuclear applications, 36th International SAMPE Technical conference*, *INEEL/CON-04-01869,* (USA, 2004)
18. V. Barabash et al., Summary of beryllium qualification activity for ITER first-wall applications. Phys. Scr. **T145**, 1–6 (2011)
19. J.F. Briesmeister, MCNP—a general Monte Carlo N-Particle Transport Code, Version 5, Los Alamos National Laboratory, (USA, 2003)
20. ITER-Final Design Report: http://www.naka.jaea.go.jp/ITER/FDR/ (2001)
21. D.L. Aldama, A. Trkov, "FENDL-2.1 Update of an evaluated nuclear data library for fusion applications", Summary documentation (2004)
22. W.M. Stacey et al., A TRU-Zr metal-fuel sodium-cooled fast subcritical advanced burner reactor. Nucl. Technol. **162**, 53–79 (2008)
23. National Research Council, *Nuclear wastes: technologies for separations and transmutations* (National Academy Press, Washington, 1996)
24. N. Demir, G. Genç, H. Yapici, Transmutation of high level wastes in a fusion-driven transmuter, *ICENES2007 13th International Conference on Emerging Nuclear Energy Systems*, (2007)
25. W.M. Stacey, *Nuclear reactor physics* (Wiley, Weinheim, 2007)
26. V. Zerkin, "ENDF/B-VII.0-USA 2006", Evaluated nuclear data file (ENDF), International Atomic Energy Agency
27. G. Piazza et al., R&D on tungsten plasma facing components for the JET ITER-like wall. J. Nucl. Mater. **367–370**, 1438–1443 (2007)
28. Luca Giacomelli, development of neutron emission spectroscopy instrumentation for deuterium and deuterium–tritium fusion plasmas at Jet, *Digital Comprehensive Summaries of Uppsala Dissertations from the Faculty of Science and Technology 339*, Uppsala University, Sweden